# Design of the Control Surfaces for an Aircraft Destined to the Competition SAE BRAZIL AERODESIGN

**Conference Paper** · January 2020

DOI: 10.4271/2019-36-0214



**6 authors**, including:

Yoko Lucila Takano e Silva
Universidade do Estado do Amazonas
**1** PUBLICATION **0** CITATIONS
SEE PROFILE

Antonio Claudio Kieling
Universidade do Estado do Amazonas
**84** PUBLICATIONS **136** CITATIONS
SEE PROFILE

Neilson Vilaça
Universidade do Estado do Amazonas
**1** PUBLICATION **0** CITATIONS
SEE PROFILE

Renan Araujo Janzen
Universidade do Estado do Amazonas
**3** PUBLICATIONS **0** CITATIONS
SEE PROFILE

SAE TECHNICAL
PAPER SERIES

2019-36-0214
E

# design of the control surfaces of an aircraft destined to the competition sae brasil aerodesign

YOKO LUCILA TAKANO E SILVA
NEILSON LUNIERE VILACA
RENAN ARAUJO JANZEN
EMILE DIANA MENDES DE AZEVEDO
SANCHES ISMAEL DE OLIVEIRA
ANTONIO CLAUDIO KIELING

SAE BRASIL

Congresso 2019 SAE BRASIL
VEÍCULOS E VIAS INTELIGENTES -
O CAMINHO PARA A MOBILIDADE SUSTENTÁVEL

SAE INTERNATIONAL

28th SAE BRASIL International
Congress and Exhibit
São Paulo, Brasil
October, 14th to 18th

AV. PAULISTA, 2073 - HORSA II - CJ. 1001 - CEP 01311-940 - SÃO PAULO – SP

2019-36-0214

# Design of the Control Surfaces for an Aircraft Destined to the Competition SAE BRAZIL AERODESIGN

**Yoko Lucila Takano e Silva, Antonio Claudio Kieling, Emile Diana Mendes de Azevedo, Neilson Luniere Vilaça, Renan Araújo Janzen, Sanches Ismael de Oliveira**

## Abstract

This work aims to present a methodology for the design of conventional control surfaces for light aircraft. Based on renowned aeronautical engineering references and standards, the theoretical framework presents the concepts of calculation for each flight phase particularity for each control surface in addition to a database with intervals of surfaces and their respective deflections of various aircraft. The methodology used takes into account the suggested steps for the aircraft design, where the dimensions are present in the preliminary design, according to the characteristics intended in the conceptual stage to develop conventional control surfaces aiming at the simplicity of design and the optimal response of control. The use of MATLAB and CFD software for data calculation and iterations are essential for the correct observance and evaluation of the obtained results. A comparative table and graphs will be elaborated for better visualization of the efficiency and behavior of each dimensioned model aiming at the best levels of acceptability according to the norms used in the design of aircraft, observing their occurrence through flight analysis and direct feedback of the pilot. Finally, the optimally sized surface will be used.

## Introduction

In an aircraft, the control surfaces are responsible for controlling the flight route. Generally, in a conventional aircraft these surfaces are as follows: (i) aileron, (ii) rudder and (iii) elevator, and this control is applied on an aircraft by the through a joystick or a pedal.

In primary control surfaces design, several factors have an effect; one of the most important is handling or flying qualities. Handling qualities are defined as “those qualities of an aircraft which governs the ease and precision with which the pilot is able to perform his mission” [1]. Maneuverability quality specifications are often expressed as (i) aircraft class, (ii) flight phases and (iii) levels of acceptability.

An aircraft is classified into four classes [4]. Class 1 represents small and light aircraft with low maneuverability, while class 2 is for medium-weight aircraft and low to medium maneuverability. Class 3 is for large, heavy aircraft and low to medium maneuverability, while Class 4 is highly maneuverable aircraft with no weight limit.

According to [2], phase A includes non-terminal flight phases that require maneuvering, precision tracking, or precise flight-path control. Phase B involves those non-terminal flight phases that are normally accomplished using gradual maneuvers and without precision tracking, although accurate flight-path control may be required. Phase C involves terminal flight phases that are normally accomplished using gradual maneuvers and usually require accurate flight-path control. In general, phases A and B are non-terminal and phase C is terminal. Phase B is usually not critical, but phases A and C, depending on the mission of the aircraft, could be critical. In designing control surfaces, only the critical phase of flight is satisfied.

Regarding the level of acceptability, this is related to the level of susceptibility of the aircraft to the ease of flight and flight safety. The level of acceptability is divided into 3, such as: (i) Flight qualities clearly adequate for the flight phase mission; (ii) Adequate flight quality to perform the mission flight, but there is some increase in the pilot's workload or degradation in the effectiveness of the mission or both; (iii) Flight qualities so that the aircraft can be safely controlled or the effectiveness of the mission is inadequate, or both [1].

## Methodology

The methodology to be used for the sizing of the control surfaces follows the proposed by [1]. First, is necessary to define what the parameters will be for scaling and what the goal will be.

On flight phases, the requirements of maneuverability qualities vary for different phases of the mission. The common categories present in every year for the SAE Brazil competition are categories B and C, which have as flight operations: landing, ascent, and descent. However, in the 2018 competition, there was a photography mission that entered category A by complexity, so for the year, it was dimensioned having all three categories as parameters.

According to [1], the control surfaces must be dimensioned so that level 1 of the maneuverability qualities is reached. Level 1 will then be taken as the goal to achieve optimal aircraft performance in the competition.

Acceptability levels may be determined based on the pilot's opinion of the aircraft's flight characteristics. It will be used the Cooper-Harper rating scale, obtaining, after each flight, the note for each command surface. It is from this rating scale that will determine if the design reached level 1 of the level of acceptability, i.e., the intended objective. Soon, Cooper-Harper's analysis will be one of the final results.

The Cooper-Harper rating scale ranges from 1 to 10, where 1 indicates the best flight characteristics and 10 the worst, as shown in the Appendix.

It was then determined that the best class for aircraft participating in the SAE Brazil competition is Class 1 because they are small. The choices are summarized in Figure 1.

After defining the three provisions for quality of maneuverability, it is necessary to define the requirements that will be applied for the sizing of the control surfaces, considering the profile of the aircraft to be dimensioned.

Following the schedule, the first command surface to be dimensioned is the aileron. The aileron is dimensioned considering the requirements of rolling control and then it is necessary to make the optimization of this one taking into account the restrictions: a vortex of wing flow, adverse yaw, and limit of deflection.

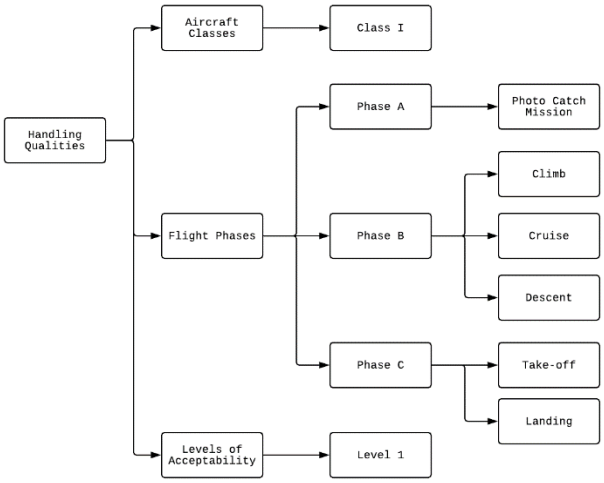


Figure 1. Certain handling qualities.

For rudder design requirements, all requirements applicable to the aircraft [1] must be analyzed given their characteristics. Therefore, the three required, observing the Urutau aircraft, are (ii) crosswind landing, (iv) coordinate curve and (v) adverse yaw, in addition to limiting the deflection limit. The adverse yaw effect has already been adjusted by the determination of aileron deflections, so the sizing focus will be on crosswind and coordinate curve, in addition to the deflection boundary constraint.

The elevator was dimensioned considering (i) rotation of takeoff and (ii) longitudinal screening, considering the deflection limit restriction, as the other two surfaces.

In addition to the Cooper-Harper analysis, the final results will also be given by the required values of the standards, to see if they are, theoretically, within that established to be considered level 1 of acceptability.

In Figure 2, the adopted methodology is presented, showing all steps of the sizing of the surfaces.

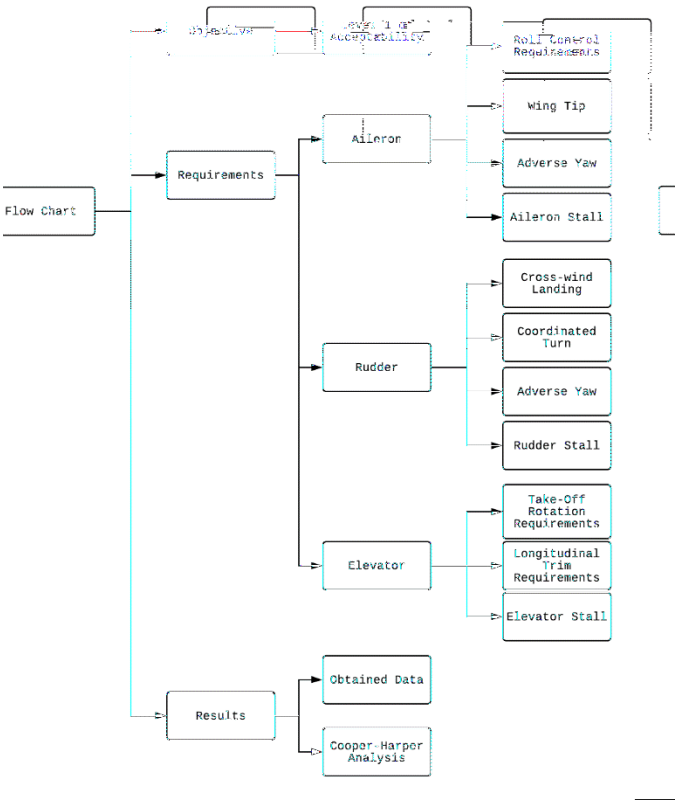


Figure 2. Adopted methodology.

## Design of Control Surfaces

### *Aileron*

According to [1], the design was done in two parts: rolling control requirements and aileron design constraints.

#### Roll Control Requirements

The rolling control requirements define the dimensioning of the aileron to achieve the bank angle variation within the duration required $t_{req}$ according to [1], shown in Table 1.

The initial calculation of $t_{req}$ used estimates from [3] to the rolling motion moment of inertia $I_{xx}$ to design the aileron. After the development of the fuselage, was obtained the real value of $I_{xx}$ that varied $t_{req}$ and invalidated the aileron in phase A (Table 2).

Besides, the first flights performed with the prototype aircraft showed that the aileron did not perform well in flight, as shown in the Cooper-Harper section. Therefore, it was necessary to resize the aileron to reach the requirement and optimize the dimensions shown in Table 3.

Table 1. Time to achieve a specified bank angle change for Class I.

| Level | Flight phase category | | |
|---|---|---|---|
| 1 | A | B | C |
| | Time to achieve a bank angle of 60º (s) | Time to achieve a bank angle of 45º (s) | Time to achieve a bank angle of 30º (s) |
| | 1,3 | 1,7 | 1,3 |

Table 2. Comparisons between moments of inertia and their respective times required

| Origination | $I_{xx}$ | $t_{req}$ |
|---|---|---|
| Reference [3] | 3,278 | 1,268 |
| Structures | 3,859 | 1,376 |

Table 3. Comparison between the time required and the calculated

| Flight Phases | A | B | C |
|---|---|---|---|
| Required | 1,3 s | 1,7 s | 1,3 s |
| Calculated | 1,263 s | 1,093 s | 0,893 s |

The formulas used to calculate the bank angle due to a rolling motion $\Phi$ and time required $t$ are shown below.

$$\Phi = \frac{I_{xx}}{\rho \cdot y_d^2 \cdot (S_w + S_h + S_{vt})} \ln(P_{ss}^2) \quad (1)$$

$$t = \sqrt{\frac{2\Phi_1}{\dot{P}}} \quad (2)$$

Where,

$\rho$ = air density

$S_w$ = planform area of wing

$S_h$ = planform area of horizontal tail

$S_{vt}$ = planform area of vertical tail

$P_{SS}$ = steady-state roll rate

$\dot{P}$ = time rate of change of the roll rate

$\Phi_1$ = bank angle when the roll rate reaches its steady-state value

$y_d$ = average distance between the rolling drag center and the aircraft center of gravity

The time required to reach the bank angle from 60º to flight phase A, meets the requirements of the standard, as shown in Figure 3.

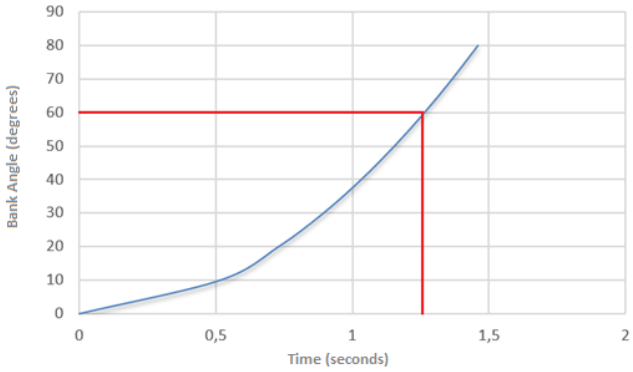


Figure 3. Relation between bank angle and time for defined aileron.

## Aileron Design Constrains

For each restriction, was proceeded as follows:

***Adverse Yaw***

The maximum deflection was selected according to historical data given by [1] and, from simulations in the XFLR5, the drag caused by this deflection was found. With the drag data, the down-deflection was found which results in this same value, removing the risk of adverse yaw caused by the aileron. Differential ailerons with values given in Table 4.

Table 4. Related values between deflection and drag

| $C_D$ | 0,024 | $\delta_{up}$ | 25º |
|---|---|---|---|
| $C_D$ | 0,024 | $\delta_{down}$ | 8º |

***Wing Tip***

Using the Autodesk CFD Plans tool and adding points of analytical coordinates, it was possible to obtain static pressure and velocity magnitude, making it easier to identify the ailerons positioning shown in figure 4.

## *Rudder*

The requirements for rudder design were determined according to [1], shown in Table 5. Since the adverse yaw requirement has already been taken into account when sizing the aileron, this rudder analysis is not required.

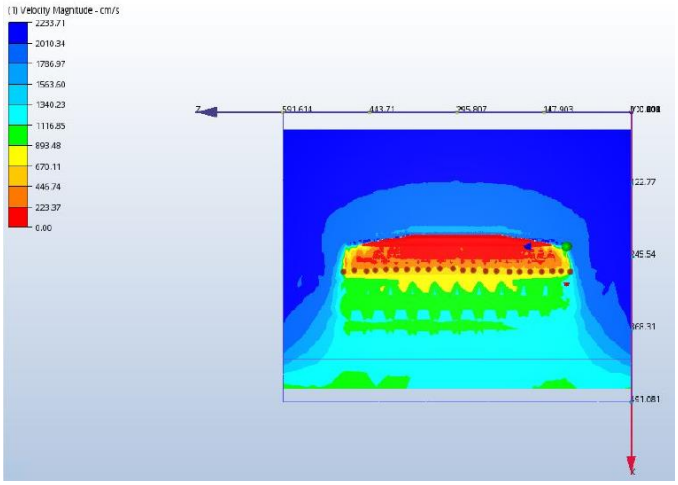


Figure 4. CFD Analysis.

Table 5. Rudder design requirements

| Requirements | Aircraft |
|---|---|
| Cross-wind landing | All |
| Coordinated turn | All |
| Adverse yaw | All |

## Coordinated Turn

After having a preliminary geometry for the rudder from [1] and after aileron design, the deflection necessary to perform a coordinate curve was analyzed.

From the simultaneous resolution between the aerodynamic side force during turn $F_{A_{y_t}}$, the aerodynamic rolling moment during turn $L_{A_t}$ and the aerodynamic rolling moment during turn $N_{A_t}$ (equations 3, 4, 5), the values of aileron deflection $\delta_A$, sideslip angle $\beta$ and rudder deflection $\delta_R$ are obtained.

$$F_{A_{y_t}} = \frac{1}{2}\rho U_1^2 S_w \left(C_{y_\beta}\beta + C_{y_r}\frac{R_1 b}{2U_1} + C_{y_{\delta_A}}\delta_A + C_{y_{\delta_R}}\delta_R\right) \quad (3)$$

$$L_{A_t} = \frac{1}{2}\rho U_1^2 S_w \left(C_{l_\beta}\beta + C_{l_r}\frac{R_1 b}{2U_1} + C_{l_{\delta_A}}\delta_A + C_{l_{\delta_R}}\delta_R\right) \quad (4)$$

$$N_{A_t} = \frac{1}{2}\rho U_1^2 S_w \left(C_{n_\beta}\beta + C_{n_r}\frac{R_1 b}{2U_1} + C_{n_{\delta_A}}\delta_A + C_{n_{\delta_R}}\delta_R\right) \quad (5)$$

Where,

$R_1$ = turn radius

$b$ = wing span

$U_1$ = aircraft forward speed

$C_{l_\beta}$ = rate of change of rolling moment coefficient with respect to sideslip angle

$C_{l_r}$ = rate of change of rolling moment coefficient with respect to yaw rate

$C_{l_{\delta_A}}$ = rate of change of rolling moment coefficient with respect to aileron deflection

$C_{l_{\delta_R}}$ = rate of change of rolling moment coefficient with respect to rudder deflection

$C_{n_\beta}$ = rate of change of yawing moment coefficient with respect to sideslip angle

$C_{n_r}$ = rate of change of yawing moment coefficient with respect to yaw rate

$C_{n_{\delta_A}}$ = rate of change of yawing moment coefficient with respect to aileron deflection

$C_{n_{\delta_R}}$ = rate of change of yawing moment coefficient with respect to rudder deflection

$C_{y_\beta}$ = rate of change in side force with respect to sideslip angle

$C_{y_r}$ = rate of change in side force with respect to yaw rate

$C_{y_{\delta_A}}$ = rate of change in side force with respect to aileron deflection

$C_{y_{\delta_R}}$ = rate of change in side force with respect to rudder deflection

The obtained rudder deflection was compared with the limit deflection of 30 ° so that there was no stall of the surface, considering Table 1 and making necessary modifications, Table 6 was obtained.

Table 6. Maximum and calculated deflection in the coordinated turn analysis

| Maximum deflection | Calculated deflection |
|---|---|
| 30º | 18º |

For security reasons the deflection was adopted for 25º.

## Cross-wind Landing

The analysis was done according to [1], considering [5], for level 1 of acceptability and for aircraft class 1, the crosswind speed value for the calculation shall be 20 knots or 10,3m/s.

By solving the two equations 6 and 7 below simultaneously, can determine two unknowns [1]: (i) rudder deflection $\delta_R$ and (ii) crab angle $\sigma$. Solving these equations simultaneously yields two unknowns. In designing the rudder, the designer should make certain that the rudder is powerful enough to allow the aircraft to land safely in a cross-wind situation.

$$\frac{1}{2}\rho V_T^2 S_w b\left[C_{n_0} + C_{n_\beta}(\beta - \sigma) + C_{n_{\delta_R}}\delta_R\right] + F_w \cdot d_c cos\sigma = 0 \quad (6)$$

$$\frac{1}{2}\rho V_W^2 S_S C_{D_y} - \frac{1}{2}\rho V_T^2 S_w\left[C_{y_0} + C_{y_\beta}(\beta - \sigma) + C_{y_{\delta_R}}\delta_R\right] = 0 \quad (7)$$

Where,

$C_{n_0}$ = residual yawing moment coefficient

$C_{y_0}$ = residual of side-force moment coefficient

$\sigma$ = sidewash angle

$V_T$ = true speed

$V_W$ = wind speed

$d_c$ = distance between the aircraft cg and the center of the projected side area of the aircraft

$F_w$ = force generated by the cross-wind

$S_S$ = aircraft projected side area

$C_{D_y}$ = aircraft side drag coefficient

The required deflection for landing is shown in Table 7, as compared to the maximum speed.

Table 7. Maximum and calculated deflection in the cross-wind landing analysis

| Maximum deflection | Calculated deflection |
|---|---|
| 30º | 15º |

After further optimizations, the final rudder configuration was determined.

However, after a strong gust wind flight, it was necessary to modify the rudder area to improve yaw control. That is, it was decided to increase the ratio between the rudder and vertical tail chord $c_R/c_v$ to 40% and increase the deflection to 30°. All previous reviews have been made again for this new helm.

The summaries of all are in Table 8.

Table 8. Maximum and calculated deflection after changes in dimensions

| Requirements | Maximum deflection | Calculated deflection |
|---|---|---|
| Coordinated turn | 30º | 17º |
| Cross-wind landing | 30º | 15º |

And the final dimensions in Table 9.

Table 9. Rudder dimensions

| | |
|---|---|
| $\delta_{R_{right}}$ | 30º |
| $\delta_{R_{left}}$ | 30º |
| $c_R$ | 0,115 m |
| $b_R$ | 0,39 m |

## *Elevator*

According to [1], considering the main wheel behind the CG, was analyzed: (i) rotation takeoff requirement and (ii) longitudinal trim requirement. According to the type of aircraft, the one shown in Table 9.

Calculating the required elevator efficiency for both requirements, $\tau_E$ = 0,803, which, on the graph, indicates the chord ratio between the elevator and the horizontal tail $c_E/c_h$ = 0.68, as shown in figure 5.

Table 10. Take-off angular acceleration requirements

| Aircraft type | Rotation time during take-off (s) | Take-off pitch angular acceleration (deg/s$^2$) |
|---|---|---|
| Remote control, model | 1 – 2 | 10 – 15 |

According to [1], an all-moving tail is recommended for ratios above 0.5 and 25 ° upward deflection. The calculations were redone by setting the string value and elevator effectiveness $\tau_E$, from equation 8, resulting in Table 11.

Both the deflection of the elevator down must be calculated as the deflection to trim the aircraft. The first one to check if it is within the maximum limit, while the second to analyze if the deflection is an expressive value because it will shatter in the loss of efficiency of the surface, since part of the deflection will be lost to balance the aircraft.

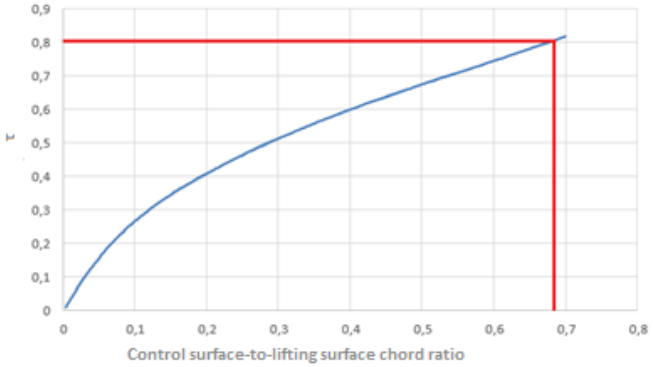

Figure 5. Control surface angle of attack effectiveness parameter.

Although the required deflection down was 2.48º, due to safety issues and geometry type values, a deflection of 10º was chosen.

Equations 9 [1] and 10 [6] were used for these calculations.

$$\tau_e = \frac{\alpha_h + \left(C_{L_h}/C_{L_{\alpha_h}}\right)}{\delta_{e_{max}}} \quad (8)$$

$$\delta_e = \frac{\left(\frac{T z_T}{\bar{q} S_w \bar{C}} + C_{m_0}\right) C_{L_\alpha} + \left(C_{L_1} - C_{L_0}\right) C_{m_\alpha}}{C_{L_\alpha} C_{m_{\delta_e}} + C_{m_\alpha} C_{L_{\delta_e}}} \quad (9)$$

$$\delta_{e_{trim}} = -\frac{C_{m_0} C_{L_\alpha} + C_{m_\alpha} C_{L_{trim}}}{C_{m_{\delta_e}} C_{L_\alpha} - C_{m_\alpha} C_{L_{\delta_e}}} \quad (10)$$

Where,

$\tau_e$ = elevator effectiveness

$\delta_e$ = elevator deflection

$\delta_{e_{trim}}$ = elevator trim angle deflection

$\alpha_h$ = tail angle of attack

$C_{L_h}$ = horizontal tail lift coefficient

$C_{L_{\alpha_h}}$ = tail lift curve slope

$\delta_{E_{max}}$ = maximum deflection of the elevator

$T$ = engine thrust

$z_T$ = offset between engine and aircraft center of gravity

$\bar{q}$ = dynamic pressure

$\bar{C}$ = mean aerodynamic chord

$C_{m_0}$ = aerodynamic pitching moment coefficient

$C_{L_\alpha}$ = lift curve slope

$C_{L_1}$ = steady-state aircraft lift coefficient

$C_{L_0}$ = aerodynamic lift moment coefficient

$C_{m_\alpha}$ = Rate of change of pitching moment with respect to angle of attack

$C_{m_{\delta_e}}$ = slope of variations of pitching moment with respect to elevator deflection.

$C_{L_{\delta_e}}$ = variation of lift coefficient versus elevator deflection

$C_{L_{trim}}$ = Lift coefficient to trim

Table 11. Elevator dimensions

| | |
|---|---|
| $\tau_E$ | 1,3 |
| $\delta_{E_{up}}$ | -25º |
| $\delta_{E_{down}}$ | 2,48º |
| $\delta_{E_{trim}}$ | 0.009º |
| $C_{m_{\delta_E}}$ | -1.867 rad-1 |
| $C_{L_{\delta_E}}$ | 0,510 rad-1 |
| $C_{L_{h_{\delta_E}}}$ | 4,7252 rad-1 |

## Elevator analysis by plotting

After the sizing of the surface, it was made the analysis, according to [2], of the variations of speed, the weight of the aircraft with payload as a function of the deflection of the surface, resulting in the following curves.

***Neutral Point***

The relationship between deflection and the variation of the position of the center of gravity is observed without the deflection of the surface being exacerbated, evidencing that the deflection of the elevator to the trim is small enough that there is no loss of effectiveness in the determined deflections.

For the plot of figure 6, equation 11 [2] was used.

Observe $\bar{h}_{PN_{ca}}$ at the intersection of the four straight lines, punctuated with the line in red. Finally, $\bar{h}_{PN_{ca}}$ = 15,83% corresponding to $\bar{h}_{PN}$ = 51.5%.

$$\delta_{e_{trim}} = -\frac{C_{m_0} - (C_L - C_{L_0})[(x_{np} - x_{CG})/\bar{c}_w]}{C_{m_{\delta_e}} + C_{L_{\delta_e}}[(x_{np} - x_{CG})/\bar{c}_w]} \quad (11)$$

Where,

$x_{np}$ = x-coordinate of the aircraft stick-fixed neutral point

$x_{CG}$ = x-coordinate of center of gravity

$\bar{c}_w$ = mean chord of the main wing

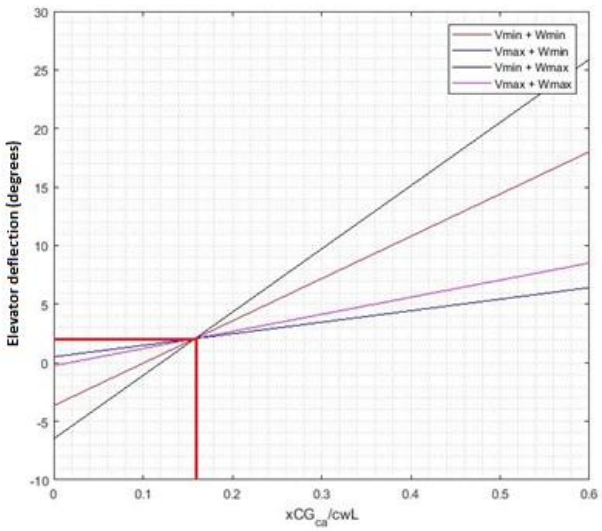


Figure 6. Relation between elevator deflection and center of gravity

***Maneuver Point***

Analyzing the elevator deflection *per g* as the load and weight variation presented in Figures 7 and 8 shows a change in the position of the maneuver point.

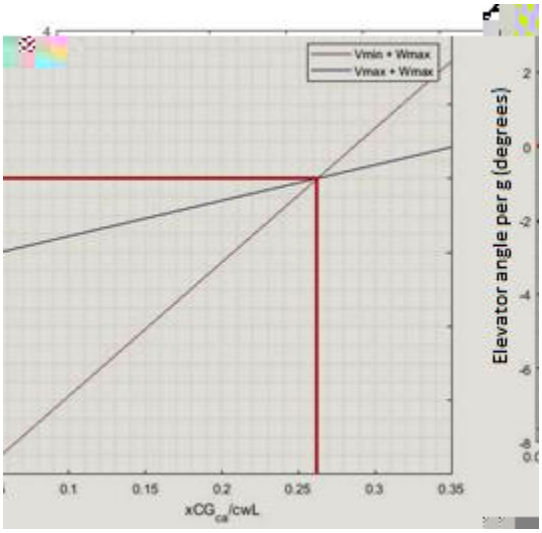


Figure 7. Relation between elevator angle *per g* and center of gravity by the maximum weight and by the modification of the speed for minimum and maximum.

For the plot of Figure 8 and 9, equation 12 [2] was used.

$$\frac{\partial \delta_e}{\partial n} = -\frac{C_W - C_{L_{\bar{q}}}\left(\frac{g\bar{c}_w}{2V^2}\right)}{C_{m_{\delta_e}} + C_{L_{\delta_e}}\left[\frac{x_{np} - x_{CG}}{\bar{c}_w}\right]}\left[\frac{C_{m_{\bar{q}}}(g\bar{c}_w/2V^2)}{C_W - C_{L_{\bar{q}}}(g\bar{c}_w/2V^2)} - \frac{x_{np}}{\bar{c}_w} + \frac{x_{CG}}{\bar{c}_w}\right] \quad (12)$$

Where,

$\partial \delta_e / \partial n$ = elevator angle per $g$

$g$ = gravitational acceleration

$C_W$ = weight coefficient

$\bar{q}$ = traditional dimensionless pitching rate

$C_{L_{\bar{q}}}$ = change in lift coefficient with respect to $\bar{q}$

$C_{m_{\bar{q}}}$ = change in pitching moment coefficient with respect to $\bar{q}$

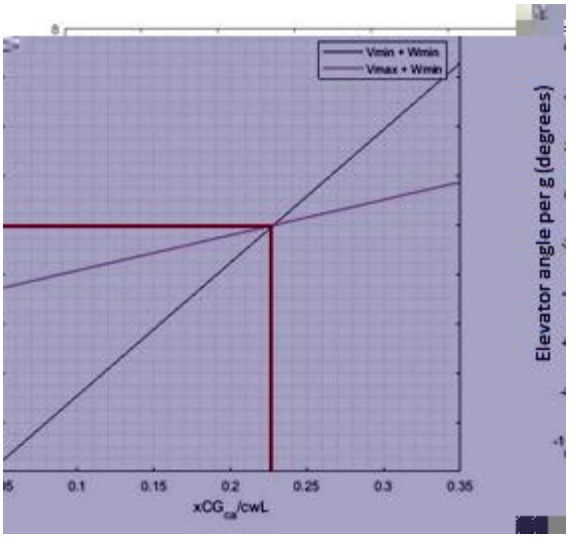


Figure 8. Relation between elevator angle *per g* and center of gravity by the minimum weight and by the modification of the speed for minimum and maximum

The red line shows the ratio of deflection angle to CG, evidencing the following positions of the maneuver point shown in table 12.

Table 12. Maneuver point.

| | |
|---|---|
| $\bar{h}_{PM}$ and $W_{min}$ | 57,84% |
| $\bar{h}_{PM}$ and $W_{max}$ | 60,33% |

***Ground Effect***

During the ground effect a variation of the maneuver point and the elevator of the required deflection. The graphical result of the ground effect can be seen in Figure 10 and Table 13.

Figure 9. Relation between elevator deflection and the center of gravity, for analysis out of ground effect and in the ground effect.

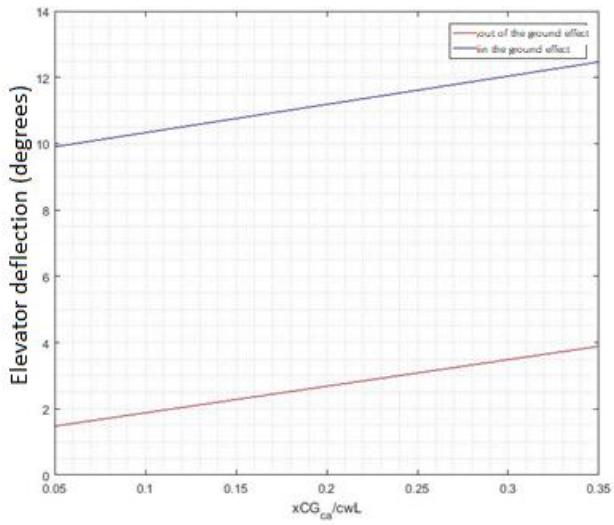


Table 13. Changes in the variables influenced by the ground effect.

| Variable | Out of the ground effect | In the ground effect |
|---|---|---|
| $\varepsilon_0$ | 0,0466 | 0,0141 |
| $d\varepsilon/d\alpha$ | 0,29859 | 0,0901 |

## Cooper-Harper Analysis

To prove that the aircraft is level 1 of acceptability for all control surfaces, was decided to use Cooper-Harper rating scale. Thus determined on the basis of the pilot's opinion.

The following Cooper-Harper analysis table for the prototype aircraft before the modifications.

Although it was scaled to, the team did not perform image capture in the competition, so it will not enter as an analysis mission for the pilot.

### *First flight*

For the first flight in a calm situation without wind gust, the Cooper-Harper rating scale is shown in Figure 14. The aircraft shows achieving level 1 of acceptability.

### *Fifth flight*

But for the fifth flight, with gust wind and rain, the efficiency of the command surfaces became inefficient, failing to achieve the desired objective. The results are shown in Table 15.

## Conclusion

To conclude that the aircraft reached level one of acceptability, that is, excellent and highly desirable characteristics, two topics should be analyzed: (i) results obtained in the dimensioning, (ii) cooper-harper handling qualities rating scale.

Although calculations focusing on level 1 of acceptability for all control surfaces, it is necessary to analyze the rates of each control surface and, if it has not reached level 1, find the reason and then correct the control surface.

On the first flight, according to the pilot, the flight performance of aileron was not satisfactory. A response delay was found on that comminuted surface. That is, to roll the aircraft, the aileron should be triggered before it can make the turn promptly. Therefore, the efficiency of the aileron should be increased.

For the elevator, since an all-moving tail was dimensioned, the surface became extremely sensitive to any movement of the control. One of the possible alternatives would be to decrease the elevator deflection angle, but another method was used.

Table 14. Rating scale for the first flight

| Flight 1 | | | |
|---|---|---|---|
| Mission | Control Surfaces | | |
| | Aileron | Rudder | Elevator |
| Takeoff | 2 | 1 | 1 |
| Cruise | 3 | 1 | 3 |
| Landing | 2 | 1 | 3 |
| Climb | 2 | 1 | 2 |
| Descent | 2 | 1 | 1 |
| Adverse yaw | 1 | 1 | |
| Cross-wind Landing | | 1 | |
| Coordinated Turn | 1 | 1 | |
| Longitudinal Trim | | | 2 |
| Rotation Takeoff | | | 1 |

Table 15. Rating scale for the fifth flight

| Flight 5 | | | |
|---|---|---|---|
| Mission | Control Surfaces | | |
| | Aileron | Rudder | Elevator |

| | | | |
|---|---|---|---|
| Takeoff | 2 | 2 | 1 |
| Cruise | 4 | 4 | 2 |
| Landing | 3 | 2 | 1 |
| Climb | 2 | 2 | 1 |
| Descent | 2 | 2 | 1 |
| Adverse yaw | 1 | 1 | |
| Cross-wind Landing | | 2 | |
| Coordinated Turn | 3 | 3 | |
| Longitudinal Trim | | | 1 |
| Rotation Takeoff | | | 1 |

The rudder, after the performance on the third flight, required a more rolling moment to perform better with gust wind.

Then, to mitigate the elevator's response problems, on the second and third flights the pilot applied the command attenuation feature in the radio software, allowing the commands to not be very sensitive to the touch, improving the response. While for aileron, the opposite feature was applied to the radio in conjunction with increasing the control surface to improve performance.

The sizing improvements to be made at the aileron and at the rudder, to improve efficiency, were to increase the area and the deflections, improving the moment of rolling and yaw respectively. With these improvements, it can be said that the sizing of the control surfaces was successful, reaching the acceptability level 1.

## References


1. Sadraey M. H., "Aircraft Design: A System Engineering Approach". 1st edition. John Wiley & Sons, 2013.
2. Phillips, W. F., "Flight Stability and Automatic Control". 2nd edition. WCB/McGraw-Hill, 1998.
3. Raymer, D.P., "Aircraft Design: A Conceptual Approach". 2nd edition. AIAA Education Series.
4. MIL-F-8785C. Military Specification: Flying Qualities of Piloted Airplanes. Department of Defense, Washington, DC, 1980.
5. MIL-STD-1797. Flying Qualities of Piloted Aircraft, Department of Defense, Washington, DC, 1997.


## Contact Information


Yoko Lucila Takano e Silva – yltes.eng@uea.edu.br

Antonio Claudio Kieling – antonio.kieling@yahoo.com

Emile Diana Mendes de Azevedo – edmda.eng@uea.edu.br

Neilson Luniere Vilaça – nlv.eng@uea.edu.br

Renan Araújo Janzen – rajn.eng16@uea.edu.br

Sanches Ismael Oliveira – sio.eng@uea.edu.br

## Appendix

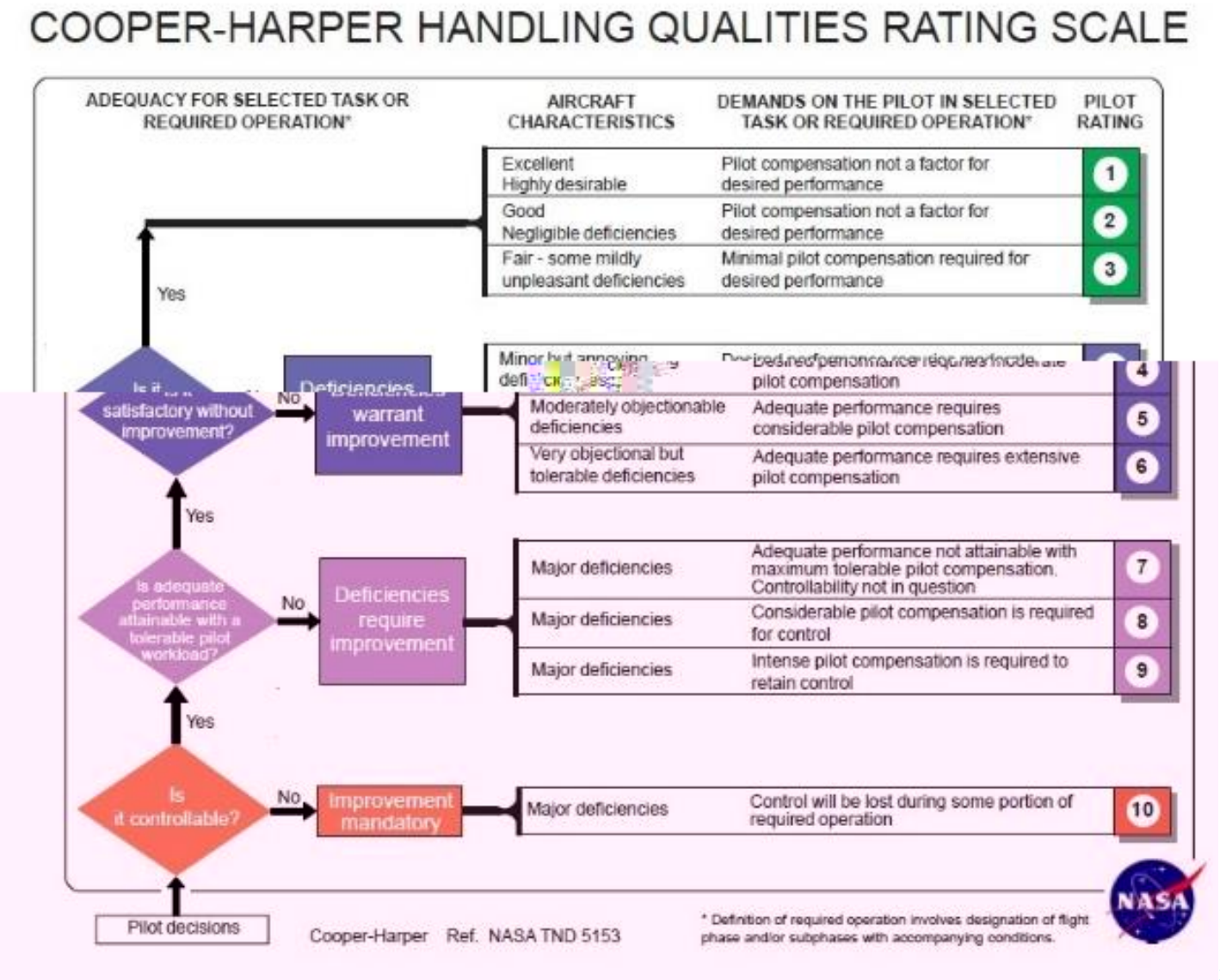


1.

igure 1. Cooper-Harper handling qualities rating scale.



**ISSN 0148-7191**